

Identification of the In Vivo Phosphorylation Sites in Murine Leukocyte-Specific Protein 1

Hongjun Shu, She Chen, Dianne DeCamp, Robert C. Hsueh, Marc Mumby, Deirdre Brekken

Alliance for Cellular Signaling Laboratories

University of Texas Southwestern Medical Center, Dallas, TX

Abstract: An abundant phosphoprotein was detected in primary B cells and WEHI-231 cells as part of a larger effort to identify ligand-induced changes in protein phosphorylation. This phosphoprotein was identified as leukocyte-specific protein-1 (LSP1), an actin-binding protein that functions in the organization of the actin cytoskeleton and cell movement. LSP1 is known to be phosphorylated in response to numerous stimuli. In this study, the two-dimensional differential gel electrophoresis system (2-D DIGE) and mass spectrometry were used to identify multiple splice variants and phosphorylated forms of LSP1 from murine primary B lymphocytes (B cells) and WEHI-231 cells. By combining 2-D DIGE with ³²P-labeling, seven phosphorylated forms of LSP1 were detected. To further characterize the phosphorylation of LSP1 in B cells, the effects of physiological stimuli and phorbol-12-myristate-13-acetate (PMA) were examined. B-cell LSP1 was found to be highly phosphorylated, even under basal conditions. LSP1 phosphorylation was strongly stimulated in response to anti-IgM and by PMA but only weakly stimulated by interleukin-4 (IL-4). Seven in vivo phosphorylation sites were detected in LSP1 using mass spectrometry. The identified phosphorylation sites include putative targets for protein kinase C, glycogen synthase kinase 3, extracellular signal-related kinase 1 (ERK1), calmodulin-dependent protein kinase 2, and mitogen-activated protein kinase-activated protein kinase 2 (MAPKAP kinase 2). The potential for phosphorylation by multiple kinases suggests that LSP1 serves as an important integration point for regulation of the actin cytoskeleton by multiple signaling pathways.

Leukocyte-specific protein 1 (also known as lymphocyte-specific protein 1, LSP1, pp52, and p50; AfCS ID A002813) is an actin-binding protein specifically expressed in B lymphocytes (B cells), T lymphocytes (T cells), macrophages, and neutrophils(1,2). LSP1 functions in the organization of the actin cytoskeleton and in cell movement. LSP1 assembles F-actin into thick, multi-branched bundles *in vitro* and coaggregates into caps with surface IgM in stimulated B cells(3). During chemotaxis in neutrophils, LSP1 colocalizes with F-actin in filopodia, lamellipodia, and membrane ruffles. Neutrophils from LSP1 knockout mice are impaired in their ability to perform chemotaxis(4), and ectopic expression of LSP1 modulates the motility of the U937 leukocyte cell line(5). LSP1 also appears to play a role in lymphocyte apoptosis(6).

The predicted size of LSP1 is 37-kDa, but the protein migrates as a 47- to 52-kDa species during sodium dodecyl sulfate-polyacrylamide gel electrophoresis (SDS-PAGE)(7). Two splice variants of LSP1 that migrate with apparent molecular masses of 50- and 52-kDa during SDS-PAGE are expressed in murine B cells. The shorter protein (324 amino acids) differs from the longer one (330 amino acids) due to deletion of a short peptide (HLIRHQ) in the central region of the molecule. Each splice variant of LSP1 migrates as multiple spots during two-dimensional gel electrophoresis, with isoelectric points ranging from pH 4.4 to 4.7 (8). There is an additional splice variant, named S37, that differs in its N-terminal amino acid sequence and is expressed in non-hematopoietic tissues(9).

LSP1 is phosphorylated in response to numerous stimuli. Phosphorylation of murine T-cell LSP1 on serine and threonine residues occurs in response to stimulation with concanavalin A or phorbol-12-myristate-13-acetate (PMA) but not with calcium ionophore(8). Peptide mapping showed that several sites phosphorylated in response to concanavalin A are phosphorylated by protein kinase C (PKC) *in vitro*(10). LSP1 is the major PKC substrate in B cells(11) and can interact directly with PKC β . PKC-mediated phosphorylation of LSP1 causes dissociation from PKC β and translocation of LSP1 from the plasma membrane to the cytosol(6,10). LSP1 is also a major substrate for mitogen-activated protein-kinase-activated protein kinase 2 (MAPKAP kinase 2) in neutrophils (12,13). Phosphorylation of LSP1 by MAPKAP kinase 2 may be part of the signaling pathway involving Rac1/Cdc42h, p21-activated kinase (PAK), p38 MAP kinase, and MAPKAP kinase 2 that regulates actin organization (14). The functional consequences of LSP1 phosphorylation are not known.

During the course of experiments to identify ligand-induced changes in protein phosphorylation in B cells, a major phosphoprotein was found in the murine WEHI-231 B lymphoma cell line and in primary murine B cells. By two-dimensional electrophoresis and mass spectrometry, this protein was identified as LSP1. Because of its potential importance as a downstream target of multiple signaling pathways, we mapped the *in vivo* phosphorylation sites on LSP1. A total of seven phosphorylation sites were detected in murine LSP1. Four of these sites were mapped to specific serine residues, and the remaining three sites were localized to specific peptide regions. This work establishes, within the Alliance for Cellular Signaling (AfCS) laboratories, the methodology for efficient identification of phosphorylation sites that will be pursued in future studies.

Results

Identification of Multiple Splice and Charge Variants of LSP1 in WEHI-231 Cells and Primary B Cells

To detect ligand-induced changes in B-cell phosphoproteins, B cells were labeled with radioactive phosphate and analyzed by two-dimensional (2-D) gel electrophoresis. Resting WEHI-231 and primary B cells were lysed in isoelectric focusing (IEF) sample buffer and proteins were resolved by 2-D electrophoresis. Images of the SYPRO Ruby-stained gels were obtained using a 2-D Image Master

fluorescence scanner and analyzed with Progenesis software to detect spots. The spot maps were filtered to remove artifactual spots caused by the presence of particulate material from the SYPRO Ruby stain. A total of 1208 and 1168 spots were detected in WEHI-231 and B cells, respectively, using a pH 4 to 7 gradient for the IEF dimension and a 12% acrylamide gel for second dimension SDS-PAGE. Although the patterns of protein spots in WEHI-231 and primary B cells were similar, there were clear differences between the two cell types (Fig. 1, panels A and B).

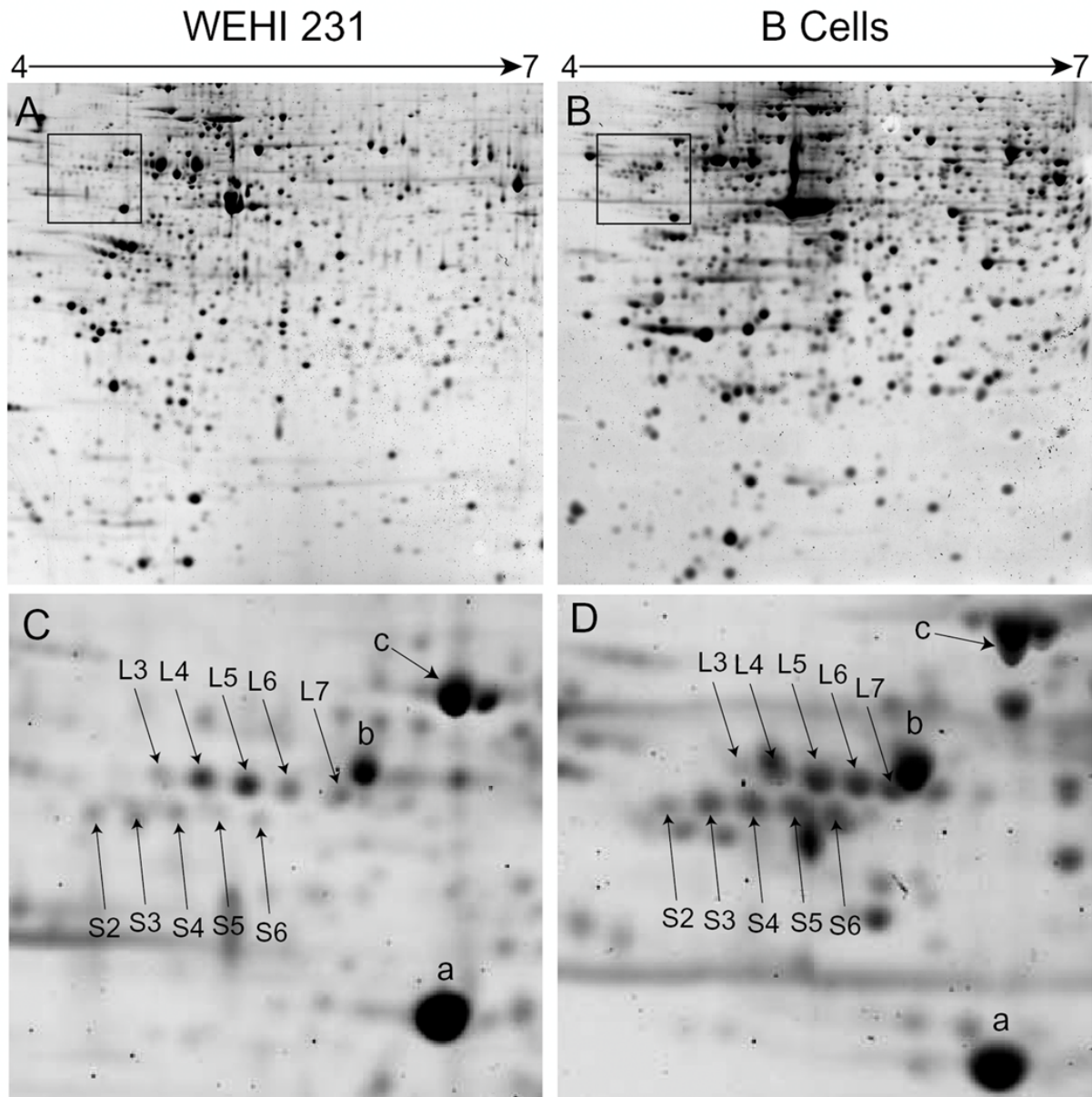


Fig. 1. Resolution of multiple charge variants of LSP1 by 2-D gel electrophoresis. Resting WEHI-231 cells and primary murine B cells were harvested and lysed using the preparative 2-D gel procedure. 500 μ g of WEHI-231 lysate (panel A) or 750 μ g of B-cell lysate (panel B) were resolved by 2-D gel electrophoresis using pH 4 to 7 gradient gels for the first dimension and 12% SDS gels for the second dimension. Following electrophoresis, the gels were fixed, stained with SYPRO Ruby, and scanned in a fluorescence imager. Panels C and D show a blown-up view of the region of the 2-D gels, outlined by boxes in panels A and B, respectively. The letters a through c in panels C and D refer to reference spots that had similar mobility in both the WEHI-231 and B-cell samples. Spots labeled L3 through L7 and S2 through S6 in panels C and D were identified as being derived from the long (L) and short (S) splice variants of LSP (GI:1346470; AfCS ID A002813).

We decided to focus on a prominent set of closely migrating phosphoproteins identified in both the WEHI-231 B lymphoma cell line and primary B cells. These prominent phosphoproteins appeared as a series of moderately abundant SYPRO Ruby-stained spots with isoelectric points between 4.4 and 4.6 and apparent molecular masses of 50- to 52-kDa. The mobilities of these spots (multiple charge variants with similar molecular weight) were consistent with the presence of differentially phosphorylated forms of single proteins. Two rows of spots (L3-L7, S2-S6) that differed by 2 to 3 kDa in apparent molecular mass were detected in both WEHI-231 and B cells (Fig. 1, panels C and D). The lower row of spots (S2-S6) was much less abundant in WEHI-231 than in B cells. The two series of spots had essentially identical isoelectric points and apparent molecular weights in the two cell types. Preparative-scale 2-D electrophoresis was then combined with mass spectrometry to identify these proteins.

Spots designated L3 to L7 and S2 to S6 in Fig. 1 were excised from preparative 2-D gels of both WEHI-231 and primary B cells and digested with trypsin. The mass spectra (MS) of the tryptic peptides and the fragments resulting from collision-activated dissociation (MS/MS) of the peptides were determined with an Applied Biosystems QSTAR Pulsar mass spectrometer equipped with a matrix-associated laser desorption ionization (MALDI) source. The MS and MS/MS data were used to search the NCBI non-redundant database using Knexus software. LSP1 was identified as the only, or the major, protein present in each of the spots analyzed (GI:1346470; AfCS ID A002813). Fig. 2 shows the MS of B-cell spots L5 and S5 as examples. Most of the MS peaks were identical in the two samples. However, a peptide with a mass-to-charge ratio (m/z) = 2107.96 was present in spot L5 but not spot S5. Conversely, a peptide with m/z = 1842.07 was present in S5, but not in L5. Comparisons of the masses of the parent peptides and fragments generated by MS/MS with the LSP1 sequence showed that these peaks corresponded to unique tryptic peptides generated from either the long (L5) or short (S5) splice variants of LSP1. The peak with m/z = 2107.96 in spot L5 was the peptide EPDPEDAVGGSGEAEEHLIR. The peak with m/z =1842.07 from spot S5 was the peptide EPDPEDAVGGSGEAEEVR. The difference between these peptides is consistent with the insertion of amino acids HLIRHQ into the long splice variant of LSP1 as reported by Matsumoto et al. (7). The same unique peptides were identified in each of the spots labeled L and S, respectively, in Fig. 1. The spots corresponding to the short splice variants in both WEHI-231 and B cells were shifted to more acidic isoelectric points relative to the long variants, consistent with the loss of a positive charge due to the absence of the arginine residue in the HLIRHQ peptide.

Apart from the unique peptides present in the long and short variants, no other differences were detected in the peptide mass fingerprints of the 10 LSP1 spots analyzed from WEHI-231 and B cells. The different forms of LSP1 resolved

in the IEF dimension were therefore due to differently charged forms of the same proteins. These observations were consistent with the presence of populations of LSP1 containing different amounts of phosphate.

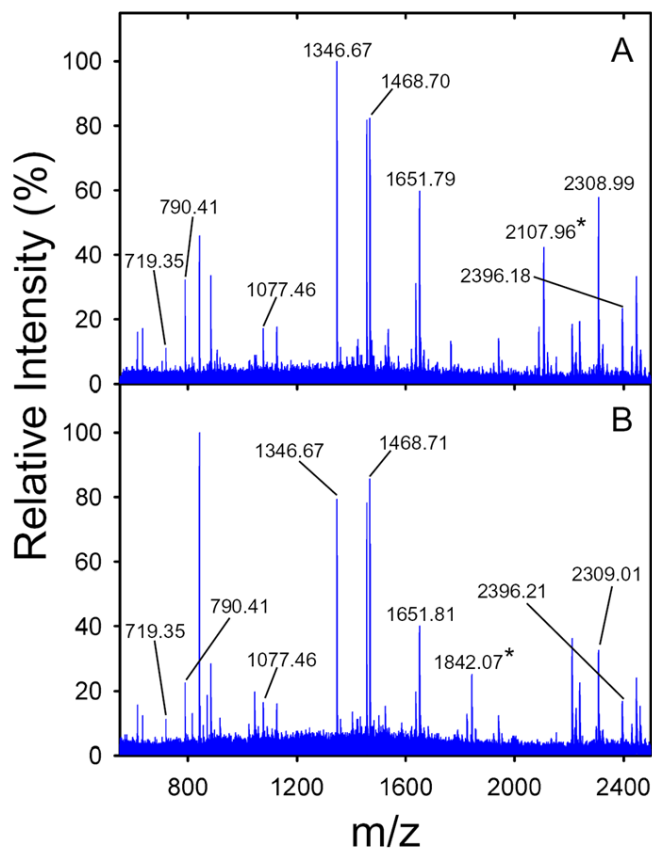


Fig. 2. Identification of the long and short splice variants of LSP1 by mass spectrometry. Spots L5 and S5 from preparative 2-D gels of B cells were excised and digested with trypsin. The masses of the tryptic peptides were determined by oMALDI-QqTOF mass spectrometry. Panel A shows the mass spectrum obtained from spot L5, and panel B shows the mass spectrum obtained from spot S5. The masses of several peptides derived from murine LSP1 that were identical between the two spots are indicated. The two peptides marked with asterisks designate peptides that were unique to spots L5 and S5, in panels A and B, respectively. These peptides uniquely identify spots L5 and S5 as the long and short variants of LSP1.

LSP1 Phosphorylation

Addition of phosphate to LSP1 should cause an increase in negative charge and shift the protein to more acidic isoelectric points. This hypothesis was tested by determining the distribution of the LSP1 spots in response to PMA treatment, a known stimulator of LSP1 phosphorylation(8). WEHI-231 cells were either left unlabeled and untreated (control) or labeled with ^{32}P inorganic phosphate and then stimulated with PMA (treated). Following lysis in IEF lysis buffer, proteins from control cells were labeled with Cy3 saturation maleimide dye and proteins in the ^{32}P -labeled, treated lysate were labeled with Cy5 dye.

Aliquots from the two lysates were mixed, and the proteins were resolved on the same 2-D gels. Following electrophoresis, images of the Cy3 and Cy5 fluorescence were obtained. The gels were then fixed and dried between pieces of cellophane. The dried gel was then placed in contact with a phosphorimager screen and held in place with tape to detect ^{32}P . After exposure, the dried gel and phosphor screen were placed together on the surface of a phosphorimager capable of scanning Cy5 fluorescence (Molecular Dynamics Storm 860). An image of the phosphor screen was obtained, followed by imaging of the Cy5 fluorescence to obtain overlapping images of the ^{32}P -labeled and fluorescently labeled proteins. This combination provided two sets of overlaid images. One set was used to compare the mobilities of the Cy3- and Cy5-labeled LSP1 protein spots in control and treated samples. The other set was used to compare the fluorescently labeled spots with the ^{32}P -labeled spots from the treated sample.

Stimulation of WEHI-231 cells with PMA resulted in an acidic shift in the LSP1 spots. Four Cy3-labeled LSP1 spots were detected in control cells (Fig. 3A). Following stimulation with PMA, six Cy5-labeled LSP1 spots were detected (Fig. 3B). Fewer total spots were detected in the fluorescent labeling experiments compared to the preparative gels shown in Fig. 1 due to differences in the lysis buffer, the amounts of protein loaded, and the fluorescent labeling of proteins. The second row of faint spots migrating above the main LSP1 spots in the PMA-stimulated sample were likely due to an artifact of the fluorescent labeling. These spots were not observed when the PMA-stimulated sample was labeled with Cy3 rather than Cy5. Since these samples were run on the same 2-D gel, the relative positions of the spots could be directly compared. Analysis of the images with DeCyder software showed that PMA stimulation resulted in an increase in the intensities of spot 3 and the appearance of two new spots (labeled 1 and 2 in Fig. 3B). The increase in the intensity of the acidic spots coincided with a decrease in the relative intensities of the basic spots (labeled 5 and 6 in Fig. 3A and 3B). The PMA-induced mobility shifts could be readily seen in a three-dimensional plot of the fluorescent image data (Fig. 3C and 3D). In Fig. 3C and 3D, a colored line is drawn around spot 4 that was detected in both the Cy3 and Cy5 images. Co-imaging of the Cy5 fluorescence and ^{32}P showed that each of the six protein-staining spots present in PMA-stimulated WEHI-231 cells coincided with a ^{32}P -labeled spot (Fig. 3E and 3F). A similar comparison showed that the four spots detected in the control lysate were also phosphorylated (not shown). These patterns of protein and ^{32}P -labeled spots indicate that LSP1 is phosphorylated at multiple sites under basal conditions. Stimulation of PKC with phorbol ester caused phosphorylation at additional sites, resulting in increased negative charge and an acidic (leftward) shift in mobility in the IEF dimension. Increased phosphorylation of LSP1 also appeared to cause a slight reduction in mobility in the SDS dimension. Based on the number of spots detected under basal and PMA-stimulated conditions, at least six phosphorylated forms of LSP1 were

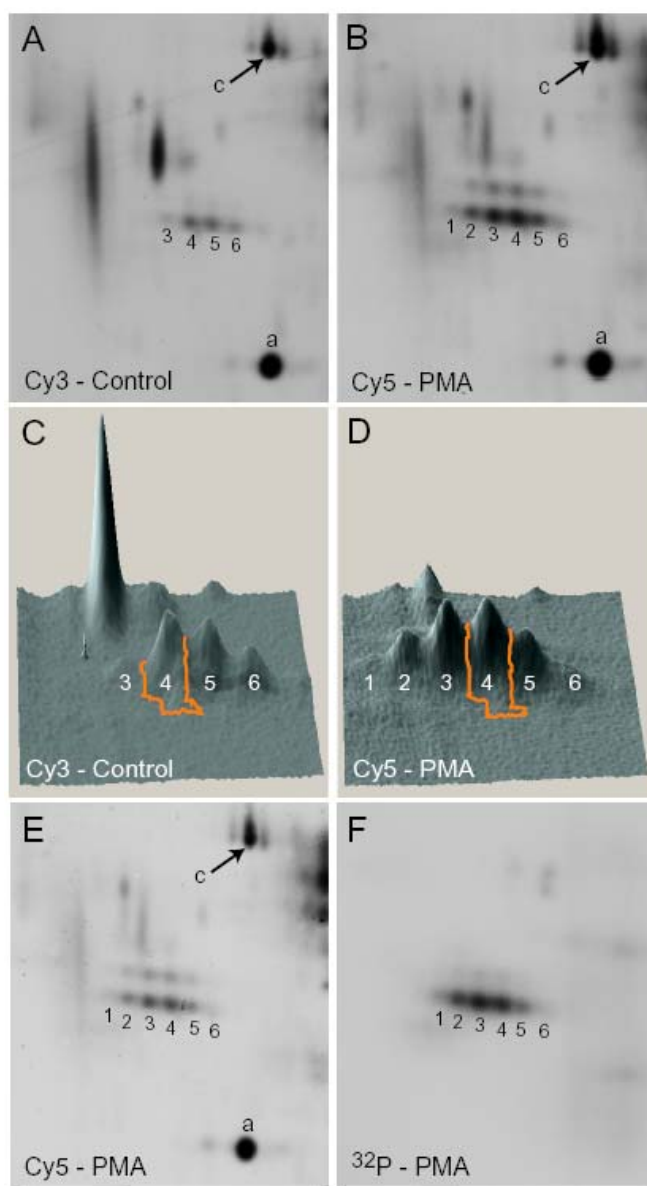


Fig. 3. LSP1 phosphorylation is enhanced by PMA stimulation. WEHI-231 cells were either unlabeled and untreated (control) or labeled with ^{32}P inorganic phosphate and stimulated for 10 min with 1 μM PMA (treated). Following lysis in IEF lysis buffer, proteins from control cells were labeled with Cy3, and proteins from the treated lysate were labeled with Cy5. Aliquots containing 10 μg of each fluorescently-labeled fraction were mixed, and proteins were resolved by 2-D gel electrophoresis. Codetection of Cy3 and Cy5, and Cy5 and ^{32}P , in the same gels was performed as described under Methods and Protocols. Panels A and B show codetected Cy3 and Cy5 images. Panels C and D show a three-dimensional representation of the images shown in A and B. Panels E and F show codetected Cy5 and ^{32}P images from the same gel. The images show the region of the 2-D gel containing the LSP1 spots and correspond to the area of the gel boxed in Fig. 1A. The pH gradient in this area ranges from pH 4.2 (on the left) to 4.8 (on the right). The lowercase letters a and c in panels A, B, and E refer to reference spots for which mobility was the same in both samples. These are the same reference spots indicated in Fig. 1C. The LSP1 spots are numbered 1 through 6 from left (more acidic) to right (less acidic). The LSP1 numbering system corresponds to that used in Fig. 1.

present in WEHI-231 cells. With higher protein loads, a seventh spot (L7) was detected (Fig. 1). These observations are consistent with previous 2-D gel data from murine T cells, indicating that LSP1 has at least six phosphorylation sites(10). With the amounts of protein loaded in this experiment, only the long splice variant of LSP1 was detected in WEHI-231 cells by either fluorescent- or ³²P-labeling.

Ligand-Induced Phosphorylation of LSP1

While the phosphorylation of LSP1 is modulated in response to several stimuli in T cells and neutrophils, pathways leading to LSP1 phosphorylation have not been as well studied in B cells. To further characterize the phosphorylation of LSP1, we examined the effects of physiological stimuli in addition to PMA. In order to obtain more quantitative measures of LSP1 phosphorylation, the ³²P contents of individual LSP1 spots were determined. WEHI-231 cells were labeled with ³²P and stimulated for 10 minutes with either PMA, anti-IgM to activate the B-cell receptor, or with interleukin-4 (IL-4). The ³²P-labeled proteins from stimulated and control cells were then resolved by 2-D gel electrophoresis. The ³²P-labeled spots corresponding to LSP1 were detected and quantitated using Progenesis software.

Seven ³²P-labeled spots with mobilities corresponding to LSP1 were detected in WEHI-231 cells. The most basic, least phosphorylated, spot (L7) was faint and only observed in control cells or cells treated with IL-4 (Fig. 4, panels A and B). Stimulation of WEHI-231 cells with IL-4 caused little change in LSP1 phosphorylation. The volumes of spots L5, L6, and L7 were slightly decreased, while the volume of spot L2 was increased (Fig. 4B and 4E). Stimulation of the B-cell receptor with anti-IgM caused a significant increase in LSP1 phosphorylation. The most basic spot (L7) disappeared, and the volumes of spots L5 and L6 were reduced relative to the controls. The volume of acidic spot L3 increased and two new acidic spots (L1 and L2) appeared (Fig. 4C and 4E). PMA-stimulation caused the greatest increase in LSP1 phosphorylation (Fig. 4D and 4E). Spots L6 and L7 were barely detectable, while the volumes of spots L1 and L2 were greatly enhanced. The similarities in LSP1 phosphorylation in response to anti-IgM and PMA are consistent with a role for PKC in phosphorylation of LSP1.

The effects of IL-4, anti-IgM, and PMA on LSP1 phosphorylation were also tested in primary B cells. Isolated B cells were cultured for 3 hours in serum-free medium containing ³²P inorganic phosphate and then stimulated with ligands for 10 minutes. The effects of stimulation on phosphorylation of the long and short forms of LSP1 were quantitated as described for WEHI-231 cells. In contrast to WEHI-231 cells, detectable levels of phosphorylation were observed in both the long and short variants of LSP1. The predominant ³²P-labeled spots in non-stimulated B cells were L3 and L4, as opposed to L4 and L5 in WEHI-231 cells, indicating that the level of LSP1 phosphorylation in resting

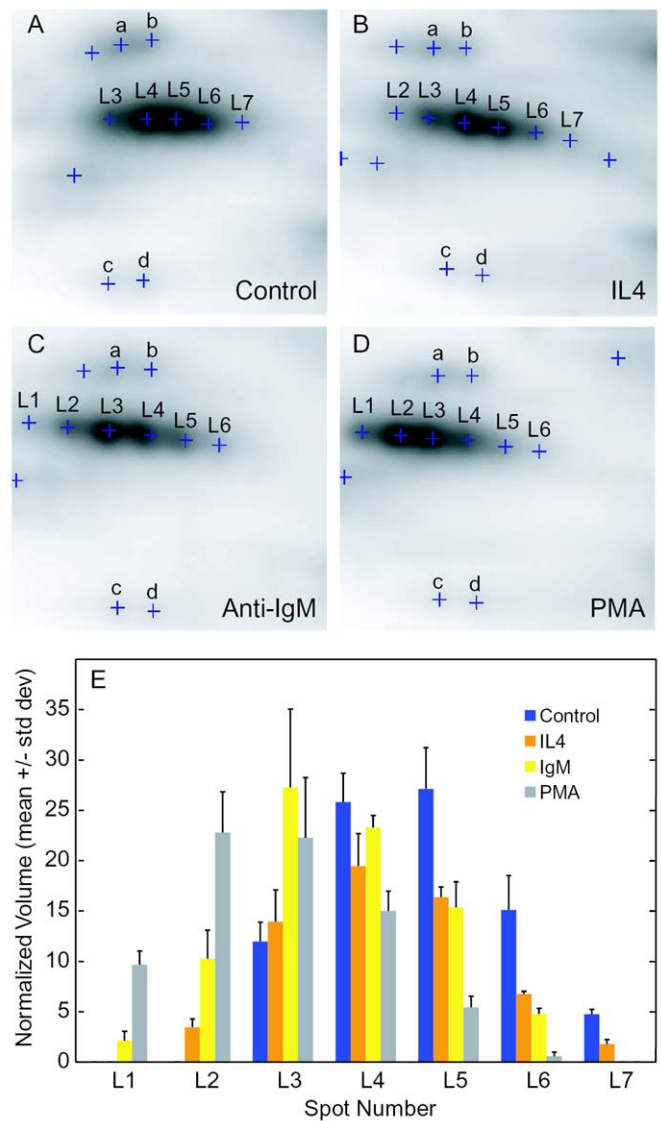


Fig. 4. Quantitative analysis of ligand-induced changes in LSP1 phosphorylation in WEHI-231 cells. WEHI-231 cells were labeled with ³²P inorganic phosphate for 3 hr and stimulated with IL-4, anti-IgM, or PMA for 10 min. Proteins were resolved by 2-D gel electrophoresis and the dried gels were exposed to phosphor screens for 72 hr. Following imaging of the phosphor screens, the ³²P-labeled spots corresponding to LSP1 were detected and quantitated with Progenesis software. The region of the 2-D gels containing the LSP1 spots from control cells (A), cells treated with IL-4 (B), cells treated with anti-IgM (C), and cells treated with PMA (D) are shown in the upper section of the figure. Spots detected by the software are labeled with blue crosses. Spots labeled L1 to L7 correspond to the different charge forms of WEHI-231 LSP1. The ³²P spots labeled a through d are reference spots for which intensities and mobilities did not change under the different conditions. Panel E shows a graph of the normalized volumes of spots L1 to L7 under the different conditions. The data shown are the mean ± standard deviation of four separate gels.

B cells was quite high. Stimulation with IL-4 had minimal if any effect on LSP1 (Fig. 5B). Stimulation with anti IgM caused an increase in phosphorylation, as observed by the appearance of new acidic spots (L1 and S1); an increase in the intensities of spots L2, L3, S2, and S3; and a decrease in the intensities of spots L6, L7, S5, and S6 (Fig. 5C). PMA treatment caused the greatest increase in phosphorylation, as judged by the increased intensities of acidic spots and decreased intensities of basic spots. Overall, the effects of ligand and PMA stimulation of primary B cells were very similar to those seen in WEHI-231 cells.

Identification of LSP1 Phosphorylation Sites

The phosphorylation sites of LSP1 were identified from samples resolved by 2-D gel electrophoresis. The LSP1 spots were excised from preparative scale 2-D gels and cleaved into peptides by in-gel digestion. Phosphorylated peptides from each spot were detected by nanospray precursor ion scanning as described in Methods and Protocols. Sample data for two WEHI-231 cell spots (L4 and L6) are shown in Fig. 6. The full mass spectrum, performed in negative ion mode, of a tryptic digest of spot L6 revealed a number of predominant peaks (Fig. 6A). Precursor ion scanning was

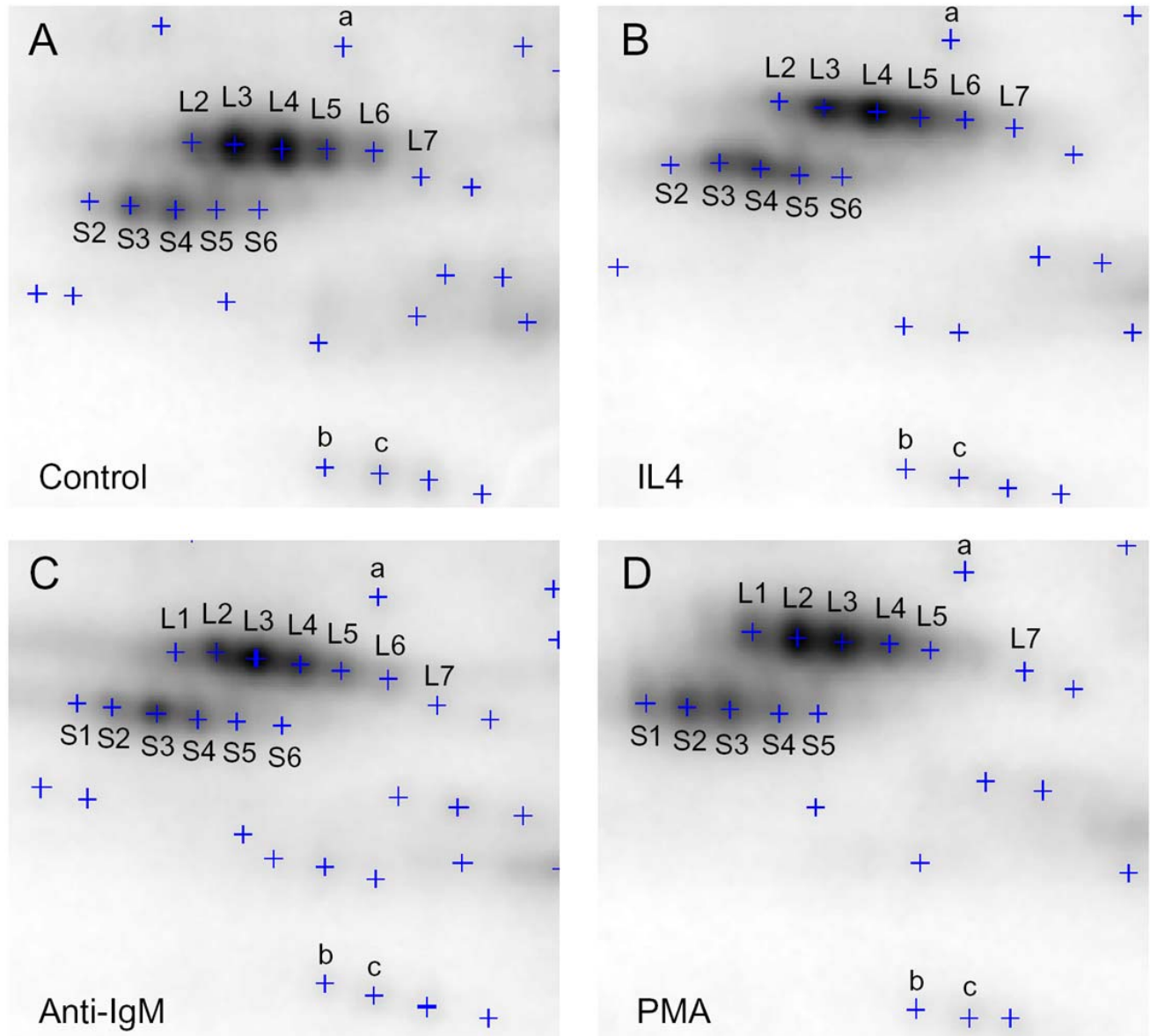


Fig. 5. Detection of ligand-induced changes in LSP1 phosphorylation in primary B cells. Primary B cells were labeled with ^{32}P inorganic phosphate and stimulated for 10 min with IL-4, anti-IgM, or PMA. Proteins were resolved by 2-D gel electrophoresis and analyzed as described for Fig. 4. Regions of the 2-D gel images containing LSP1 from control (A), IL-4-stimulated (B), anti-IgM-stimulated (C), and PMA-stimulated (D) cells are shown. The ^{32}P spots detected by Progenesis software are marked by a blue cross. Spots labeled L1 to L7 and S1 to S6 correspond to the different charge forms of the long and short splice variants of LSP1, respectively. Spots labeled a, b, and c are reference spots that had similar mobilities under all conditions.

then used to detect the m/z -79 (PO^3^-) product ions released during MS/MS. A large number of phosphorylated peptide ions were detected in spot L6 (Fig. 6B). Most of the phosphopeptides were either minor components or undetectable in the full mass spectrum. The phosphorylated peptides were all present as multiply charged species, leading to the plethora of detectable peaks. A total of four phosphorylated peptide ions were detected (labeled T1, T2, T4, and T5 in Fig. 6B). As expected, the full mass spectrum of the tryptic peptides derived from spot L4 (a more highly phosphorylated species) was essentially identical to that of spot L6 (compare Fig. 6C and 6A). Precursor ion scanning of spot L4 detected two peptides (T1 and T2) that were also detected in spot L6 (Fig. 6D). Phosphopeptide T3, which was not detected in spot L6 (Fig. 6B), was a predominant phosphopeptide in spot L4 (Fig. 6D). In contrast, phosphopeptides T4 and T5 appeared to be absent in spot L4. As shown below, peptides T3, T4, and T5 are differentially phosphorylated forms of the same tryptic peptide (Table 1). Spot L4 contains the quadruply phosphorylated form of the peptide (T3), and spot L6 contains the doubly (T5) and triply (T4) phosphorylated forms of the peptide. These observations suggest that an important component in the acidic shift of spot L4 relative to L6 is due to phosphorylation of additional sites within this tryptic peptide. In order to cover more of the LSP1 sequence and identify additional phosphorylation sites, the LSP1 spots were also digested with Glu-C protease. The results of Glu-C digestion of spot L6 are shown in Fig. 6E and 6F. As observed following tryptic digestion, the phosphorylated peptides detected by precursor ion scanning were not readily detectable in the full mass spectrum (Fig. 6E and 6F). A total of five phosphorylated Glu-C peptides were detected in spot L6. These represented a total of four distinct peptides. Peptides G3 and G4 differed by a single amino acid due to cleavage at adjacent glutamic acid residues (Table 1).

Ten phosphorylated peptide ions were detected by precursor ion scanning of tryptic and Glu C peptides derived from LSP1. This represented a total of six distinct peptides after taking differential modifications into account. The representative data shown in Fig. 6 were derived from LSP1 spots L4 and L6 from WEHI-231 cells. Precursor ion scanning was also performed on spots L5 and L7 from both WEHI-231 and B cells and spots L4 and L6 from B cells. While the numbers of phosphopeptides detected varied between spots, the same phosphopeptides found in spot L4 were also found in the other spots. No additional phosphopeptides were detected indicating that each spot contained the same set of phosphopeptides. Fewer phosphopeptides were detected in spots L6 and L7, which would be consistent with a lower level of phosphorylation. However, the non-quantitative nature of the mass spectrometry analysis precludes making any conclusions about whether sites in LSP1 are phosphorylated in a random or a hierarchical manner.

After identification of phosphorylated peptides by precursor ion scanning, individual phosphorylation sites were identified by nanospray tandem mass spectrometry. Once the m/z ratios of phosphopeptides were determined by precursor ion scanning in negative ion mode, the peptide (precursor) ions at the corresponding m/z values in positive ion mode were fragmented by collision-induced dissociation. The resulting MS of the product ions provided partial sequence information that was used to identify the sites of phosphorylation. In most cases, a signal for the precursor ions was not visible in the positive mode MS scan. Nevertheless, fragmentation at the appropriate m/z value gave clear product ion spectra derived from the correct peptide. Whenever possible, tandem mass spectrometry was performed on both the doubly and triply charged forms of the precursor ions. Product ion spectra for tryptic peptide T2

Table 1. Summary of phosphopeptides and phosphorylation sites identified in murine LSP1. This table lists the phosphopeptides and the phosphorylation sites identified in LSP1. Modifications include phosphorylation (P) and methionine oxidation (O). Modified residues are preceded by a lower case letter and are underlined.

Peptide	Mass	Modifications	Sequence	Residues	Phosphorylation Sites
T1	1637.81	1P	QPpSIELPSMAVASTK	241-255	Ser-243
T2	1653.81	1P + 1O	QPpSIELPSoMAVASTK	241-255	Ser-243
T3	2699.24	4P	TPSPLALEDTVELSSPPLSPTTK	166-188	Unassigned
T4	2619.24	3P	TPSPLALEDTVELSSPPLSPTTK	166-188	Unassigned
T5	2539.24	2P	TPSPLALEDTVELSSPPLSPTTK	166-188	Unassigned
G1	2949.59	1P	SLNRSIKKSNpSVKKSQPTLP I STIDE	195-220	Ser-205
G2	1971.97	2P	LSpSPPLpSPTTKLADRTE	178-194	Ser-180, Ser-184
G3	2599.29	2P	EHLIRHQVRTPSPLALEDTVE	157-177	Unassigned
G4	2470.25	2P	HLIRHQVRTPSPLALEDTVE	158-177	Unassigned
G5	1951.96	1P	QPGQQTLISLKSSE	66-82	Unassigned

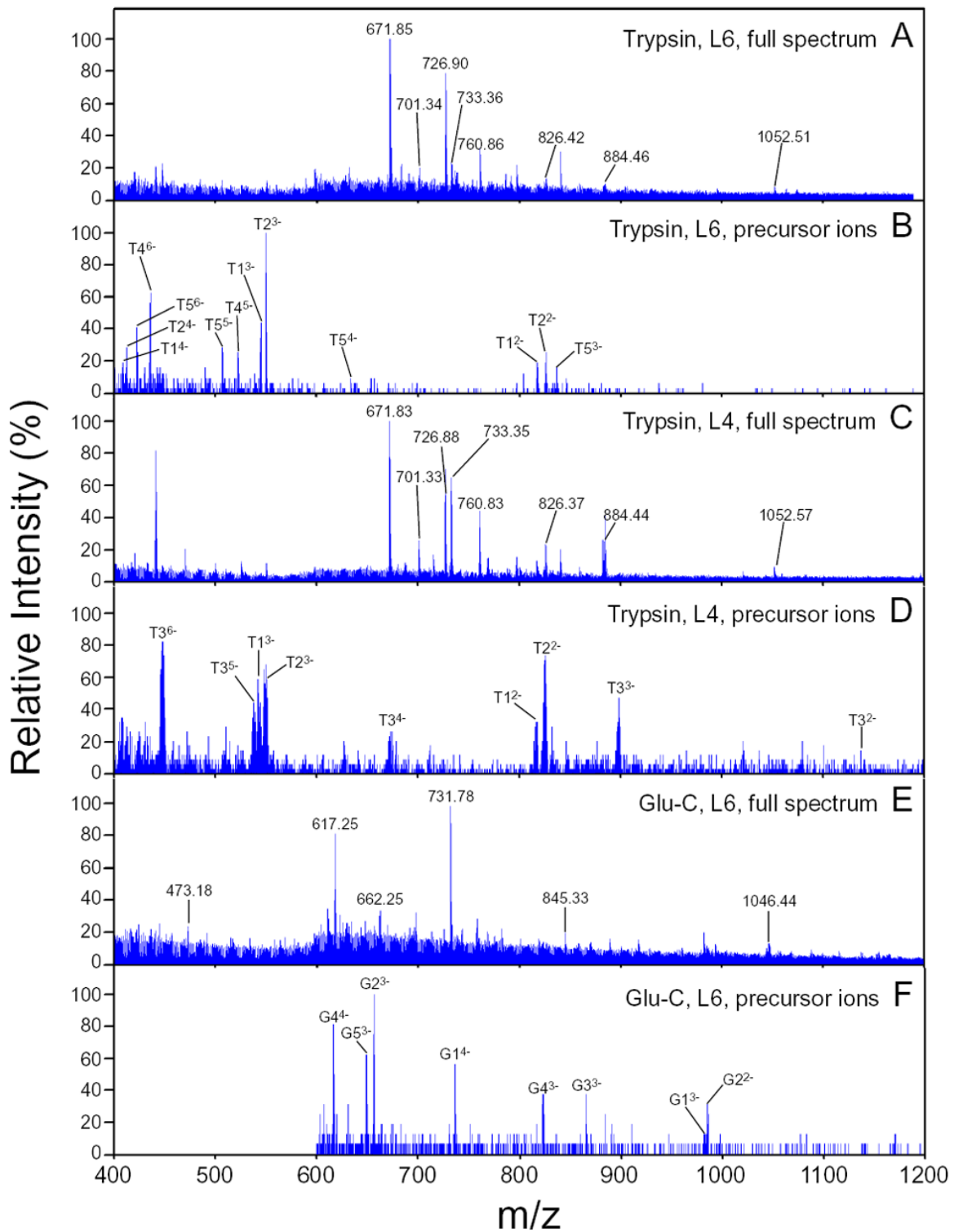


Fig. 6. Identification of phosphorylated LSP1 peptides by precursor ion scanning. WEHI-231 LSP1 was resolved by preparative 2-D gel electrophoresis. Spots L4 and L6 of LSP1 were excised from 2-D gels and digested with either trypsin or Glu-C protease. The resulting peptide mixtures were analyzed by precursor ion scanning using nanospray mass spectrometry in negative ion mode. (A) Full mass spectrum of the tryptic digest of spot L6. (B) Precursor ion scan of the tryptic digest of spot L6. (C) Full mass spectrum of the tryptic digest of spot L4. (D) Precursor ion scan of the tryptic digest of spot L4. Panel E; full mass spectrum of the Glu-C digest of spot L6. (F) Precursor ion scan of the Glu-C digest of spot L6; due to limited amounts of sample, MS data were only collected for m/z 600 to 1200. In panels A, C, and E, the major LSP1 peptide ions are labeled with their m/z values. In panels B, D, and F, the major phosphate-containing peptide ions detected in the precursor scan are labeled with a number corresponding to the peptide from which the ions were derived (T1 to T5 are tryptic peptides; G1 to G5 are Glu-C peptides). The charge states (2- to 6-) of the peptide ions detected in the precursor scans are indicated by superscript numbers.

from WEHI-231 spot L4, Glu-C peptide G1 from WEHI-231 spot L4, and Glu-C peptide G2 from B-cell spot L4 are shown in Fig. 7. The partial sequence data obtained allowed assignment of four phosphorylation sites in these three peptides (Table 1). Peptides T1 and T2 were identical except for the presence of oxidized methionine in T2 (a common artifact seen in mass spectrometry). Tandem mass spectrometry of peptide T1 identified Ser-243 as the phosphorylation site in this tryptic peptide (not shown). Phosphorylation sites at Ser-180, Ser-184, and Ser-205 were identified from the product ion spectra of Glu-C peptides G1 and G2. As discussed above, peptides T3 through T5 were differentially phosphorylated forms of the same peptide (amino acids 166-188). As summarized in Table 1, the product ion spectra of these peptides indicated a total of four phosphorylation sites (data not shown). However, the spectra contained insufficient information to assign these sites due to the low abundance of the precursor ions. The product ion spectrum of Glu-C peptide G2, which overlapped with the C-terminal region of the 166-188 tryptic peptide, allowed identification of Ser-180 and Ser-184 as two of the four sites phosphorylated. The product ion spectra of Glu-C peptide G3/G4, which overlap with the amino terminal region of the 166-188 tryptic peptide, both contained two phosphates that could not be assigned. The G3/G4 peptide (157-EHLIRHQVRTPSPLALEDTVE-177) contains two threonines and one serine (indicated by asterisks in Fig. 8). The product ion spectrum of peptide G5 identified an additional phosphorylation site in an amino terminal LSP1 peptide (66-QPGQQLISLKSSE-82). Although precursor ions from this peptide were analyzed multiple times, unambiguous assignment of the phosphorylation site was not possible. The four potential phosphorylation sites in this peptide are indicated by asterisks in Fig. 8.

The collection of 10 phosphorylated peptides from LSP1 identified a total of 7 sites of phosphorylation. Four of these were assigned to Ser-180, Ser-184, Ser-205, and Ser-243 (Fig. 8). Two of the remaining sites were localized to a Glu-C peptide containing Thr-166, Ser-168, and Thr-175. The final site was localized to a Glu-C peptide containing Thr-71, Ser-74, Ser-77, and Ser-78. The presence of seven phosphorylation sites is consistent with the resolution of LSP1 into seven charge forms by 2-D electrophoresis. The fact that these sites were all identified in resting cells indicates that LSP1 is highly phosphorylated under basal conditions. A total of 64% of the LSP1 sequence was covered by the tryptic and Glu-C peptides identified in these experiments. A significant number of serine, threonine, and tyrosine residues are present in peptides that were not detected, and LSP1 could contain additional sites of phosphorylation.

To determine if the phosphorylation sites identified here might be substrates for known protein kinases, predicted sites of phosphorylation of LSP1 were identified by analyzing the LSP1 amino acid sequence with NetPhos (www.cbs.dtu.dk/services/NetPhos/), PROSITE (www.expasy.ch/prosite/), and Scansite (<http://scansite.mit.edu>) phosphorylation site prediction programs. The results of these searches are shown

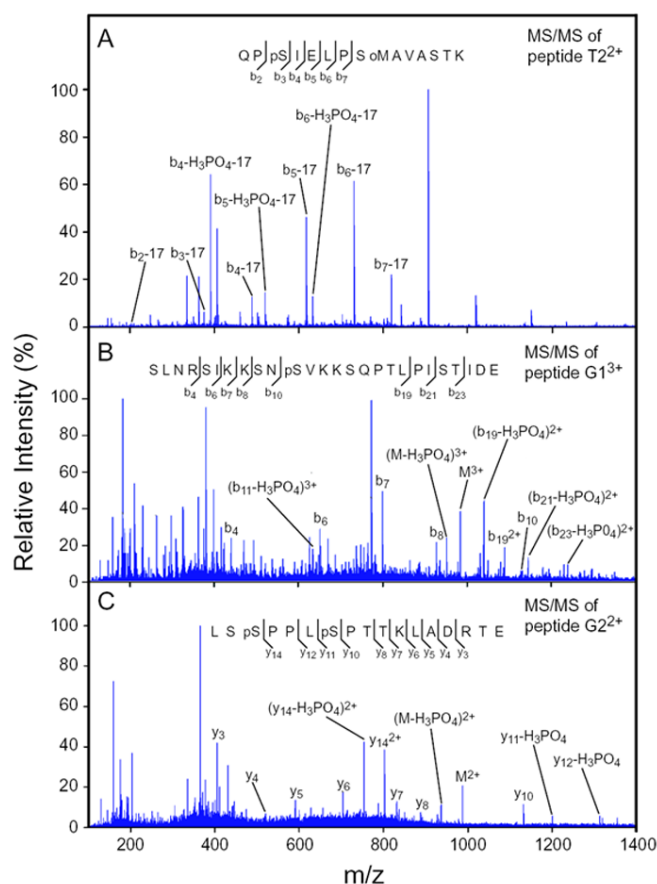


Fig. 7. Identification of LSP1 phosphorylation sites by tandem mass spectrometry. Proteolytic digests of LSP1 were prepared as described for Fig. 6 and analyzed by tandem mass spectrometry. Following identification of phosphorylated peptides by precursor ion scanning in negative ion mode, peptide ions at the corresponding m/z values were analyzed by tandem mass spectrometry in positive ion mode. The MS of the product ions resulting from collision-induced dissociation of LSP1 peptides is shown. The product ion peaks (either b series or y series) that were most diagnostic of the phosphorylation sites are indicated along with the sequence of the peptide. The fragments representing individual b or y ions are indicated by lines between the corresponding amino acids. The charge states of the product ions are indicated in superscript. Ions with no superscript numbers are singly charged. In several cases, peaks corresponding to product ions containing phosphate (b_n or y_n), and satellite peaks resulting from neutral loss (98 Da) of phosphoric acid ($b_n-H_3PO_4$ or $y_n-H_3PO_4$) were detected. (A) Product ion spectrum of the doubly charged tryptic peptide T2 precursor ion at m/z 819.9 from WEHI-231. In addition to neutral loss of phosphoric acid, all of the product ions labeled in this spectrum had masses that were 17 Da lower than the actual mass due to the neutral loss of $[NH_3]$. (B) Product ion spectrum of the triply charged Glu-C peptide G1 precursor ion from WEHI-231 at m/z 984.2. In addition to product ions, the mass spectrum also contains a peak corresponding to the triply charged precursor ion (M^{3+}) and a satellite peak resulting from neutral loss of phosphoric acid at m/z 935.2 ($M-H_3PO_4$)³⁺. (C) Product ion spectrum of the doubly charged Glu-C peptide G2 precursor ion at m/z 987.0 from B cells. This spectrum also contains a peak corresponding to the precursor ion (M^{2+}) and a peak resulting from neutral loss of phosphoric acid ($M-H_3PO_4$)²⁺.

MAEAAIDPRC EEQEELHAED SEGLTTQWRE EDEEEAAREQ RQRERERQLQ 50
 DQDKDKEDDG GHSLEQPGQQ *TLI*SLK*SEL DEDEGFGDWS QKPEPRQQFW 100
 GNEGTAEGTE PSQSERPEEK QTEESSHQAK VHLEESNLSY REPDPEDAVG 150
 GSGEAEHLI RHQVRT*PSPL ALED*TVELSS PPLSPTTKLA DRTESLNRSI 200
 KKSNSVKKSQ PTLPISTIDE RLQYQTQATE SSGRTPKLSR QPSIELPSMA 250
 VASTKTLWET GEVQSQSASK TPSCQDIVAG DMSKKSLEWEG KGGSKISSSTI 300
 KSTPSGKRYK FVATGHGKYE KVLVDEGSAP 330

Fig. 8. Summary of the phosphorylation sites identified in LSP1. The amino acid sequence of the long splice variant of murine LSP1 is shown. Orange underlining indicates the tryptic peptides that were identified. Blue underlining indicates the Glu-C peptides identified. Residues identified as phosphorylation sites are in boldfaced type and marked with the amino acid residue number. Possible phosphorylated residues within peptides where the actual sites could not be identified are marked by asterisks. These included a single phosphorylation site within peptide G5 (residues 66-82) and two phosphorylation sites within peptide G3/G4 (residues 157-177).

in Table 2. All four of the directly identified sites (Ser-180, Ser-184, Ser-205, and Ser-243) were predicted to be sites of phosphorylation by both NetPhos and Scansite. While PROSITE predicted Ser-205 to be a PKC site, the other sites were not predicted to be phosphorylated. This is likely due to the limited number of kinase phosphorylation site motifs included in PROSITE. Ser-205 was predicted to be a PKC site by both PROSITE and Scansite and is very likely to be an *in vivo* site of PKC phosphorylation. Ser-243 had a very low Scansite percentile score as a site for calmodulin-dependent protein kinase 2 (CaMKII) indicating a close match to the optimal sequence. This residue was previously proposed to be a MAPKAP kinase 2 phosphorylation site(12). While Ser-184 was a predicted site for several proline-directed kinases, only ERK1 had a Scansite percentile score below the standard cutoff of 0.2(15). Of the putative kinase motifs containing Ser-180, only GSK3 had a Scansite percentile score below 0.2. There were no obvious candidate protein kinases for the phosphorylation sites present in peptides G3/G4 or G5. Of the three possible phosphorylation sites on Glu-C peptide G3/G4, only Ser-168 was predicted as a phosphorylation site by NetPhos. Of the four possible sites in peptide G5, Ser-78 had the highest NetPhos score. While it is not clear how accurate these predictions will be, they suggest that LSP1 is likely to be a substrate of multiple protein kinases including CaMKII, GSK3, MAPKAP kinase 2, PKC, and ERK1.

Discussion

LSP1 was detected as a relatively abundant phosphoprotein in primary B cells and WEHI-231 cells as part of a larger effort to identify ligand-induced changes in protein phosphorylation. Because previous work indicated it was a target of multiple signaling pathways, it was important to identify the sites on LSP1 that are phosphorylated in intact cells. The availability of sensitive mass spectrometry methods made it possible to accomplish this with small amounts of material (e.g., approximately 1 pmol of protein per 2-D spot) resolved from whole cell lysates by 2-D gel electrophoresis. Both the long and short splice variants of LSP1 were present as multiply charged variants that were separated during 2-D electrophoresis. The long splice variant was resolved into seven spots and the short variant into six spots. Each of the

Table 2. Comparison of identified LSP1 phosphorylation sites with sites predicted by motif scanning programs. The murine LSP1 amino acid sequence was used to identify predicted phosphorylation sites using the NetPhos (www.cbs.dtu.dk/services/NetPhos/), PROSITE (www.expasy.ch/prosite/), and Scansite (<http://scansite.mit.edu>) phosphorylation site prediction programs. The NetPhos data show whether the identified sites were predicted (+) or not predicted (-) to be sites of phosphorylation. For those sites that were predicted, the NetPhos score is given in parentheses. The closer the NetPhos score is to 1, the more likely the site represents an actual phosphorylation site(17). For those sites predicted by PROSITE, the predicted protein kinase is shown and those not predicted are indicated by (-). For sites predicted by Scansite, the protein kinases predicted to phosphorylate that site are listed and those not predicted are indicated by (-). The sites predicted by Scansite, set at medium stringency, are followed by the percentile ranking of the candidate motif with respect to all potential motifs in the Swiss-Prot database(15). The closer the percentile ranking is to 0, the closer the sequence is to the optimal motif. Sites with percentile ranks less than 0.1 for that kinase are listed in boldfaced type.

Site	NetPhos	PROSITE	Scansite
Thr-71*	-	-	CaMKII (0.671)
Ser-74*	+ (0.925)	PKC	-
Ser-77*	+ (0.802)	-	-
Ser-78*	+ (0.996)	CK2	-
Thr-166†	-	-	-
Ser-168†	+ (0.950)	-	-
Thr-175†	-	-	-
Ser-180	+ (0.925)	-	GSK3 (0.189) p38 MAPK (0.676) ERK1 (0.480)
Ser-184	+ (0.995)	-	GSK3 (0.276) CDK5 (0.881) CDC2 (0.421) ERK1 (0.020)
Ser-205	+ (0.996)	PKC	PKC $\alpha/\beta/\gamma$ (0.024) PKC δ (0.527)
Ser-243	+ (0.978)	-	CaMKII (0.069)

*These sites are the possible phosphorylation sites in peptide G5. The mass spectrometry data indicated that only one of these sites was phosphorylated.

†These sites are the possible phosphorylation sites in peptide G3/G4. The mass spectrometry data indicated that two of these sites were phosphorylated.

spots was labeled with ^{32}P , indicating that they were all phosphorylated forms of LSP1. Multiple phosphorylation is supported by previous studies in which immunoprecipitated T-cell LSP1 was treated with alkaline phosphatase and analyzed by 2-D electrophoresis(7). B-cell LSP1 was highly phosphorylated even under basal conditions. In quiescent B cells cultured for 3 hours in serum-free medium, the predominant forms of LSP1 were those containing 4 and 5 moles of phosphate. LSP1 from WEHI-231 cells cultured in serum-free medium was predominantly present as forms containing 3 and 4 moles of phosphate. Previous studies have also shown a significant level of basal LSP1 phosphorylation in BAL17 B lymphoma cells(16), primary murine T cells (8), human B cells, and the human CESS B lymphoblastoid cell line(11). However, cells in these studies were cultured in the presence of 10% fetal bovine serum, which could have caused increased levels of LSP1 phosphorylation.

The phosphorylation of LSP1 in WEHI-231 and primary B cells was differentially affected by ligands. Stimulation of B cells with a concentration of IL-4 that elicited a robust response in the [AfCS B-cell ligand screen](#) had modest effects on LSP1 phosphorylation. In contrast, activation of the B-cell receptor with anti-IgM antibody or stimulation of PKC with PMA caused a significant increase in LSP1 phosphorylation. In WEHI-231 cells, stimulation resulted in a shift in the intensities of either fluorescent- or ^{32}P -labeled spots to the more acidic forms. Similar results were observed in primary B cells. In each case, the effects of PMA were stronger than those resulting from activation of the B-cell receptor. These data are consistent with previous results, indicating an important role for PKC in ligand-induced LSP1 phosphorylation(8,11). However, other protein kinases are also likely to play a role in LSP1 phosphorylation. For example, human neutrophil LSP1 is phosphorylated *in vitro* by MAPKAP kinase 2, and introduction of a MAPKAP kinase 2 inhibitory peptide into intact neutrophils repressed LSP1 phosphorylation induced by PMA or fMet-Leu-Phe(13).

A total of seven *in vivo* phosphorylation sites were detected in LSP1 by mass spectrometry based methods (summarized in Fig. 8). This number is in concordance with the resolution of LSP1 into at least seven charged species by isoelectric focusing. These results suggest that most, or all, of the major sites of phosphorylation were identified. However, coverage of the LSP1 sequence by the peptides identified here was not complete, and additional sites could be present. Although the role of phosphorylation in regulating the function of LSP1 is unknown, the data provided here show that LSP1 is phosphorylated at multiple sites *in vivo*. Two of the phosphorylation sites we identified, Ser-205 and Ser-243, are located within the caldesmon-like domain of the protein, and two of the sites, Ser-180 and Ser-184, are immediately adjacent to this domain(18). It is possible that the phosphorylation of these sites may alter the interaction of LSP1 with actin or other proteins. The potential to be phosphorylated by multiple kinases raises the possibility that LSP1 serves as an important integration point for regulation of the actin cytoskeleton by multiple signaling pathways.

Important goals for the future are to identify the protein kinases responsible for phosphorylating LSP1 *in vivo* and to determine how phosphorylation at each site affects the function of LSP1. On a broader scale, this work establishes a reproducible protocol for using 2-D gels and mass spectrometry for the determination of phosphorylation sites in future experiments by the AfCS.

Methods and Protocols

Detailed methods and protocols used for these studies are available in PDF format and are accessible via the online version of this report. Additions or modifications to standard methods are described below.

Preparative 2-D Gel Electrophoresis

WEHI-231 cells (1.5×10^7) were grown in medium containing fetal bovine serum. Primary splenic B cells (1.5×10^8) were isolated as described above (PP00000001) and incubated for 1 hour in serum-free Dulbecco's Modified Eagle's Medium (DMEM). Cells were collected by centrifugation and washed once with phosphate buffered saline. The cell pellets were lysed with IEF lysis buffer (8M urea, 4% CHAPS, 20mM Tris-HCl, pH 9, 5 $\mu\text{l/ml}$ Pefabloc, 1X Complete Mini Protease Cocktail [Roche], 1mM sodium orthovanadate, 1 μM okadaic acid) at a ratio of 50 μl of buffer per 1×10^7 cells. The lysates were then sonicated 2 times for 3 seconds and ultracentrifuged for 1 hour at 22°C at 70,000 x g. The protein in the supernatant was precipitated with TCA/acetone and resuspended in rehydration buffer (8M urea, 4% CHAPS, 1% immobilized pH gradient [IPG] buffer, 13 mM DTT, 5 $\mu\text{l/ml}$ Pefabloc, 1X Complete Mini Protease Cocktail [Roche], 1mM sodium orthovanadate, 1 μM okadaic acid). The proteins were then separated by 2-D electrophoresis (protocols available on the AfCS Web site). The standard protocols were followed, except the glass plates were treated with Bind Silane (Amersham Biosciences) before gel casting to keep the gel attached to the plate during spot picking. Preparative 2-D gels were stained with either Colloidal Blue (Invitrogen) or SYPRO Ruby (Bio-Rad) according to the manufacturer's protocols. The gels were then imaged in a 2-D Master Imager fluorescence scanner (Amersham Biosciences).

Mass Spectrometry

The Colloidal Blue- or SYPRO Ruby-stained LSP1 protein spots were excised and digested according to the AfCS protocol (PP00000156). The MS and MS/MS spectra were acquired by oMALDI-QqTOF mass spectrometry (PP00000157). The MS and MS/MS spectra were used to search the NCBI non-redundant mouse protein database using Knexus software (Genomic Solutions, Inc.). Nano-electrospray precursor ion scanning and tandem mass spectrometry (MS/MS) (PP00000158) were used to identify phosphorylation sites in LSP1. The phosphorylation sites were identified by manual analysis of the fragmentation patterns of individual phosphopeptides.

Analytical 2-D Gel Electrophoresis

WEHI-231 cells (1.1×10^7) were incubated in phosphate-free Supplemented Iscove's Modified Dulbecco's Medium (SIMDM), and primary B cells (2×10^7) were incubated in phosphate-free DMEM media, both containing 1 mCi/ml of ^{32}P inorganic phosphate, for 3 hours at 37°C in 5% CO_2 . Cells were then treated with anti-IgM, IL-4 or PMA for 10 minutes according to AfCS protocols. Cells were collected by centrifugation.

For fluorescent labeling, the cell pellet was lysed with TTX-1 IEF lysis buffer (50 mM Tris-HCl, pH 7.6, 300 mM NaCl, 0.5% Triton X-100, 1X complete protease inhibitor cocktail [Roche], 1 mM sodium orthovanadate, 1 μM okadaic acid) at a ratio of 10 μl of buffer per 1×10^6 cells. The lysate was incubated on ice for 30 minutes with occasional vortexing. The sample was then centrifuged for 15 minutes at 12,000 x g at 4°C. The proteins were labeled with Cy3 or Cy5 dyes* (Amersham Biosciences) according to the AfCS protocol (PP00000150), TCA precipitated, and resuspended in 2-D rehydration buffer 1 (AfCS protocol PS00000481) for 2-D electrophoresis.

For samples that were not fluorescently labeled, the cell pellet was lysed with TriPure at a ratio of 10 μl of buffer per 1×10^6 cells, followed by protein extraction according to the AfCS protocol (PP00000154). The protein pellets were resuspended in 2-D rehydration buffer 1 for 2-D electrophoresis.

*We used Cy3 and Cy5 saturation dyes from Amersham Biosciences, available only to customers with a technology access agreement with Amersham. Amersham Biosciences recommends Cy3 minimal dye (catalog no. RPK0273) and Cy5 minimal dye (catalog no. RPK0275) as commercially available substitutes for the saturation dyes. These substitutes were not tested by the AfCS; therefore we cannot predict if these substitutes will produce identical results to those detailed in this report.

References

- Li Y, Guerrero A, and Howard TH. (1995) *J. Immunol.* 155(7), 3563-3569.
- Pulford K, Jones M, Banham AH, Haralambieva E, and Mason DY. (1999) *Immunology* 96(2), 262-271.
- Klein DP, Galea S, and Jongstra J. (1990) *J. Immunol.* 145(9), 2967-2973.
- Hannigan M, Zhan L, Ai Y, and Huang CK. (2001) *J. Leukoc. Biol.* 69(3), 497-504.
- Li Y, Zhang Q, Aaron R, Hilliard L, and Howard TH. (2000) *Blood* 96(3), 1100-1105.
- Cao MY, Shinjo F, Heinrichs S, Soh JW, Jongstra-Bilen J, and Jongstra J. (2001) *J. Biol. Chem.* 276(27), 24506-24510.
- Matsumoto N, Kita K, Kojima S, et al. (1995) *J. Biochem.(Tokyo)* 118(1), 237-243.
- Matsumoto N, Toyoshima S, and Osawa T. (1993) *J. Biochem.(Tokyo)* 113(5), 630-636.
- Gimble JM, Dorheim MA, Youkhana K, et al. (1993) *J. Immunol* 150(1), 115-121
- Matsumoto N, Kojima S, Osawa T, and Toyoshima S. (1995) *J. Biochem.(Tokyo)* 117(1), 222-229.
- Carballo E, Colomer D, Vives-Corrons JL, Blackshear PJ, and Gil J. (1996) *J. Immunol.* 156(5), 1709-1713.
- Huang CK, Zhan L, Ai Y, and Jongstra J. (1997) *J. Biol. Chem.* 272(1), 17-19.
- Zu YL, Ai Y, Gilchrist A, Labadia ME, Sha'afi RI, and Huang CK. (1996) *Blood* 87(12), 5287-5296.
- Bagrodia S, Derijard B, Davis RJ, and Cerione RA. (1995) *J. Biol. Chem.* 270(47), 27995-27998.
- Yaffe MB, Leparo GG, Lai J, Obata T, Volinia S, and Cantley LC. (2001) *Nat. Biotechnol.* 19(4), 348-353.
- Jongstra-Bilen J, Wielowieyski A, Misener V, and Jongstra J. (1999) *Mol. Immunol.* 36(6), 349-359.
- Blom N, Gammeltoft S, and Brunak S. (1999) *J. Mol. Biol.* 294(5), 1351-1362.
- Zhang Q, Li Y, and Howard TH. (2000) *J. Immunol.* 165(4), 2052-2058. Blom N, Gammeltoft S, and Brunak S. (1999) *J. Mol. Biol.* 294(5), 1351-1362.

Authors*

Hongjun Shu^{†‡}
She Chen[‡]
Dianne DeCamp[‡]
Robert C. Hsueh[§]
Marc Mumby[‡]
Deirdre Brekken^{†‡}

Acknowledgements

Technical Assistance
Farah El Mazouni[†]
Victor Galanis[‡]
Kathleen Lyon[‡]
Sivasakthy Sivalogan[‡]

Editors

Ashley K. Butler
Duke University, Durham, NC

Gilberto R. Sambrano^{||}
University of California San Francisco, San Francisco, CA

Reviewers

Lewis Cantley
Harvard Medical School, Boston, MA

Michael Gold
University of British Columbia, Vancouver, BC

* Please refer to the AfCS policy on [authorship](#).

† To whom scientific correspondence should be addressed.

‡ Protein Chemistry Laboratory, University of Texas Southwestern Medical Center, Dallas, TX.

§ Cell Preparation and Analysis Laboratory, University of Texas Southwestern Medical Center, Dallas, TX.

|| To whom questions or comments about the AfCS Research Reports should be addressed.